12. T. M. Panhuis, R. Butlin, M. Zuk, T. Tregenza, *Trends Ecol. Evol.* **16**, 364 (2001).
13. G. S. van Doorn, U. Dieckmann, F. J. Weissing, *Am. Nat.* **163**, 709 (2004).
14. M. E. Arnegard, A. S. Kondrashov, *Evolution* **58**, 222 (2004).
15. M. Andersson, L. W. Simmons, *Trends Ecol. Evol.* **21**, 296 (2006).
16. M. Kirkpatrick, M. J. Ryan, *Nature* **350**, 33 (1991).
17. Y. Iwasa, A. Pomiankowski, S. Nee, *Evolution* **45**, 1431 (1991).
18. M. D. Jennions, A. P. Møller, M. Petrie, *Q. Rev. Biol.* **76**, 3 (2001).
19. M. D. Jennions, M. Petrie, *Biol. Rev. Cambridge Philos. Soc.* **75**, 21 (2000).
20. A. P. Møller, R. V. Alatalo, *Proc. R. Soc. London Ser. B Biol. Sci.* **266**, 85 (1999).
21. H. Levene, *Am. Nat.* **87**, 331 (1953).
22. R. A. Johnstone, *Biol. Rev. Cambridge Philos. Soc.* **70**, 1 (1995).
23. S. Cotton, K. Fowler, A. Pomiankowski, *Proc. R. Soc. London Ser. B Biol. Sci.* **271**, 771 (2004).
24. E. S. Dolgin, M. C. Whitlock, A. F. Agrawal, *J. Evol. Biol.* **19**, 1894 (2006).
25. P. D. Lorch, S. Proulx, L. Rowe, T. Day, *Evol. Ecol. Res.* **5**, 867 (2003).
26. S. R. Proulx, *Evolution* **55**, 2401 (2001).
27. K. Reinhold, *Org. Diversity Evol.* **4**, 157 (2004).
28. P. Edelaar, A. M. Siepielski, J. Clobert, *Evolution* **62**, 2462 (2008).
29. L. F. Bussière, J. Hunt, K. N. Stolting, M. D. Jennions, R. Brooks, *Genetica* **134**, 69 (2008).
30. H. Kokko, K. Heubel, *Genetica* **134**, 55 (2008).
31. This work was supported by a Rubicon grant from the Netherlands Organization for Scientific Research (G.S.v.D.) and a European Commission Marie Curie Outgoing International Fellowship grant (P.E.). This paper reflects the authors' opinion only. We thank A. Leeuw for exploratory simulations; D. Visser for creating Fig. 1; and I. Olivieri, T. van Dooren, M. Maan, and two anonymous reviewers for constructive comments.

Supporting Online Material
www.sciencemag.org/cgi/content/full/1181661/DC1
SOM Text
Figs. S1 to S3
References and Notes

8 September 2009; accepted 26 October 2009
Published online 26 November 2009;
10.1126/science.1181661
Include this information when citing this paper.

Structure of the LKB1-STRAD-MO25 Complex Reveals an Allosteric Mechanism of Kinase Activation

Elton Zeqiraj,[1,2] Beatrice Maria Filippi,[2] Maria Deak,[2] Dario R. Alessi,[2] Daan M. F. van Aalten[1]*

The LKB1 tumor suppressor is a protein kinase that controls the activity of adenosine monophosphate–activated protein kinase (AMPK). LKB1 activity is regulated by the pseudokinase STRADα and the scaffolding protein MO25α through an unknown, phosphorylation-independent, mechanism. We describe the structure of the core heterotrimeric LKB1-STRADα-MO25α complex, revealing an unusual allosteric mechanism of LKB1 activation. STRADα adopts a closed conformation typical of active protein kinases and binds LKB1 as a pseudosubstrate. STRADα and MO25α promote the active conformation of LKB1, which is stabilized by MO25α interacting with the LKB1 activation loop. This previously undescribed mechanism of kinase activation may be relevant to understanding the evolution of other pseudokinases. The structure also reveals how mutations found in Peutz-Jeghers syndrome and in various sporadic cancers impair LKB1 function.

Loss-of-function mutations in the tumor suppressor LKB1 cause the rare inherited disease Peutz-Jeghers syndrome (PJS) in humans (*1*) and are associated with various sporadic cancers, in particular non–small cell lung cancer (*2*). One prominent function of LKB1 is to ensure that growth and division are coupled to the availability of cellular energy. LKB1 phosphorylates and activates the adenosine monophosphate–activated protein kinase (AMPK) when energy levels are low, thereby leading to inhibition of signaling pathways that promote proliferation (*3*). The therapeutic effects of AMPK-activating drugs (e.g., metformin) on tumor growth (*4*) or blood glucose levels (*5*) are dependent on activation of AMPK by LKB1. Another key role of LKB1 is to control cell polarity, which may be mediated by AMPK (*6*) or by a group of AMPK-related protein kinases, including microtubule affinity-regulating kinases (MARKs, homologous to the *Caenorhabditis elegans* kinase Par-1) (*7*) that are also phosphorylated and activated by LKB1 (*8*).

In cells, LKB1 is found in a 1:1:1 heterotrimeric complex with the pseudokinase STRAD (Ste20-related adaptor) (*9*) and the scaffolding MO25 (mouse protein 25) (*10*). There are two closely related human isoforms of both STRAD (STRADα and STRADβ) and MO25 (MO25α and MO25β) that similarly interact with LKB1 (*11*). Unlike the majority of protein kinases, which are regulated by phosphorylation, LKB1 is activated by binding to STRAD and MO25 (*11*, *12*) through an unknown, phosphorylation-independent, molecular mechanism. Structural analysis of MO25α reveals a helical-repeat, horseshoe-shaped protein that interacts with the C-terminal WEF (Trp-Glu-Phe) motif of STRADα through a hydrophobic pocket located on its convex C-terminal surface (*13*). The structure of STRADα complexed with MO25α reveals additional interactions between the concave surface of MO25α and the regulatory αC helix of STRADα (*14*). STRADα, despite being a catalytically inactive pseudokinase, adopts a closed conformation typical of fully active protein kinases. The closed conformation of STRADα is maintained through its cooperative binding to adenosine triphosphate (ATP) and MO25α. Mutations that inhibit binding to ATP and MO25α prevent LKB1 activation, which suggests that the active conformational state of STRADα may be required for activation of LKB1 (*14*).

We report the crystal structure of the LKB1-STRADα-MO25α heterotrimeric complex. We used an insect cell expression system to produce an active core LKB1-STRADα-MO25α heterotrimeric complex, comprising the kinase domain of LKB1 (residues 43 to 347), complexed with the pseudokinase domain of STRADα (residues 59 to 431) and full-length MO25α (figs. S1 and S2). The crystal structure of the heterotrimeric complex with a catalytically inactive mutant of LKB1 ($Asp^{194} \rightarrow Ala$, preventing Mg^{2+} ion binding but not assembly of the complex; fig. S2B) in complex with the ATP analog adenyl-5′-yl imidodiphosphate (AMP-PNP) was solved and refined to 2.65 Å (table S1). There are two heterotrimeric complexes in the asymmetric unit displaying similar conformations (RMSD = 0.5 Å on 791 Cα atoms). Both STRADα and LKB1 are in complex with AMP-PNP, displaying binding modes typical of other protein kinases (fig. S3) (*15*).

The LKB1 heterotrimer has an overall compact globular shape with considerable interactions among all of the three subunits (Fig. 1A and fig. S4). The pseudokinase domain of STRADα binds to the kinase domain of LKB1. The horseshoe-shaped MO25α acts as a scaffold for assembly of the heterotrimer by binding both LKB1 and STRADα through highly conserved residues on the concave face of its helical repeats (Fig. 1A and fig. S4B). MO25α binds to STRADα through a large (2930 $Å^2$) interface centered on the regulatory helix αC of STRADα (Fig. 1A). The structure of the STRADα-MO25α complex within the heterotrimer is similar to the binary STRADα-MO25α complex structure (*14*) (RMSD = 0.5 Å on 529 Cα atoms; fig. S5), including ordered electron density for the STRADα C-terminal WEF motif interacting with a pocket on MO25α (*13*, *14*). The remaining MO25α concave surface is engaged in contacts (1580 $Å^2$) with the LKB1 activation loop, helix αI, and the C terminus of helix αC (Fig. 1A and fig. S4). The interface between LKB1 and STRADα mainly involves the C lobe of STRADα and both N and C lobes of LKB1 (1840 $Å^2$; Fig. 1C and fig. S4) and is comparable in size to the interaction between LKB1 and MO25α.

[1]Division of Molecular Microbiology, College of Life Sciences, University of Dundee, Dundee DD1 5EH, Scotland. [2]MRC Protein Phosphorylation Unit, College of Life Sciences, University of Dundee, Dundee DD1 5EH, Scotland.

*To whom correspondence should be addressed. E-mail: dmfvanaalten@dundee.ac.uk

Activation of LKB1 is thought to be mediated through a conformational change triggered by binding to STRAD and MO25 (*11*, *12*). The structure of the core LKB1 heterotrimer is consistent with this, as LKB1 lacks phosphorylation of the activation loop yet adopts an active conformation (fig. S6). The LKB1 αC helix is rotated into the canonical closed conformation, forming the conserved salt bridge between Lys^{78} (the so-called VAIK motif in subdomain II) and Glu^{98} (αC helix in subdomain III; fig. S6). This active conformation of LKB1 appears to be achieved through contributions of both STRADα and MO25α.

Structural elements on the STRADα C lobe that normally make up the substrate binding site in active protein kinases [i.e., the αG helix (*16*) and the p+1 loop (*15*)] interact with LKB1 (Fig. 1B and fig. S7). Furthermore, the activation loop of STRADα interacts with both N and C lobes of the LKB1 kinase domain (Fig. 1B). Mutation of residues in the substrate-binding region of STRADα (Leu^{241} in the p+1 loop and Gln^{251} in the αEF-αF loop) inhibit interaction with LKB1, whereas mutation of Gln^{286} (αG helix) has a moderate effect (Fig. 2A). Mutation of Gln^{251} (αEF-αF loop), alone or in combination with a mutation on STRADα that disrupts the MO25α-STRADα interaction (Tyr^{185} → Phe) (*14*), suppresses LKB1 activation without affecting complex assembly (Fig. 2B). The reciprocal mutation of Arg^{74} on LKB1 that forms a hydrogen bond to Gln^{251} (Fig. 1B) also impairs the ability of STRADα to activate LKB1 without affecting complex assembly (Fig. 2D). These experiments suggest that binding of STRADα to the β2-β3 loop of LKB1 exerts a conformational effect that promotes LKB1 activation.

Comparison of the active and inactive structures of cyclin-dependent kinase 2 and epidermal growth factor receptor reveals that the β2-β3 loop undergoes large positional shift upon activation (fig. S8). Furthermore, β2-β3 loop interactions of RAF are important for its dimerization-dependent activation (*17*) (fig. S8C). Interestingly, residues on the STRADα activation loop (His^{231} and Phe^{233}) bind to β7-β8 (C lobe) and β2-β3 (N lobe) of LKB1, respectively (Fig. 1B), perhaps aiding in the positioning of the N and C lobes relative to each other. In the absence of MO25α, mutation of His^{231}, Phe^{233}, or both prevented STRADα from binding to LKB1 (Fig. 2A). However, in the presence of MO25α, only the His^{231}-Phe^{233} double mutant reduced LKB1 activation and complex

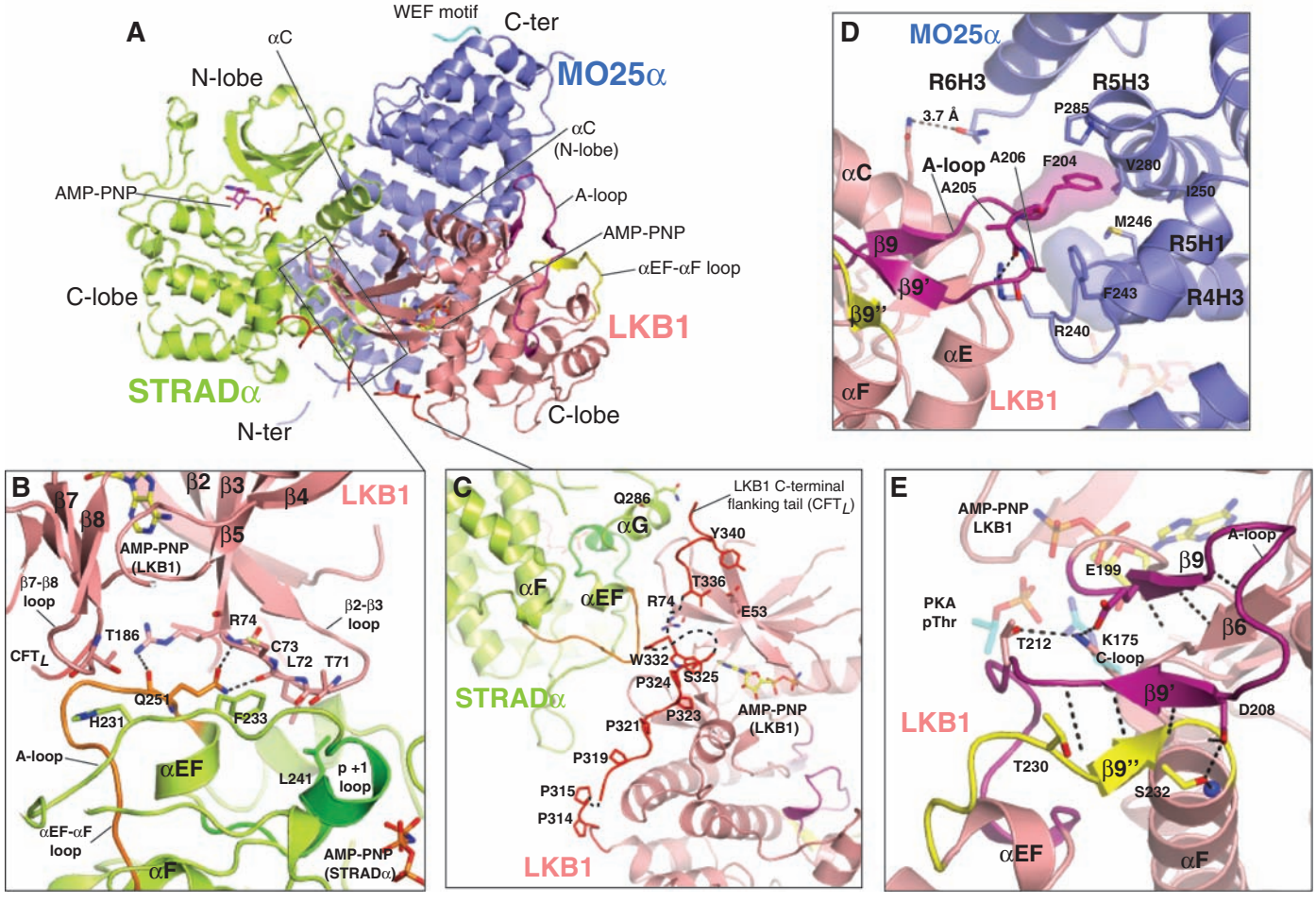

Fig. 1. Overall structure and LKB1-STRADα-MO25α complex interactions. (**A**) Cartoon representation of the heterotrimeric complex and two bound AMP-PNP molecules are shown in stick representations (LKB1, yellow carbons; STRADα, magenta carbons). The γ-P for AMP-PNP bound to LKB1 was not visible because of disorder. The WEF motif at the C terminus of STRADα, for which connectivity could not be unambiguously identified because of disorder of the linkers, is shown in cyan. (**B**) Detailed view of LKB1-STRADα interaction. STRADα p+1 and αEF-αF loops are colored green and orange, respectively. (**C**) Interaction of the LKB1 CFT_L with STRADα and LKB1 N and C lobes. The proline-rich CFT_L is colored red. (**D**) Detailed view of LKB1-MO25α interaction. The LKB1 activation loop is colored magenta. (**E**) Detailed view of LKB1 A-loop interactions. Backbone interactions are shown as dashed lines. Residues Asp^{208}, Thr^{230}, and Ser^{232} mutated in PJS are labeled and their side chains displayed. A salt bridge between Glu^{199} and Lys^{175} (dashed line) represents the interaction of the LKB1 activation segment with its catalytic loop (C-loop). The corresponding interaction found in PKA (PDB ID 1ATP) between the phosphorylated Thr^{197} (pThr) and Arg^{165} is also shown, with PKA residues represented as transparent sticks (carbon atoms colored cyan). The typical "activatory" threonine (Thr^{202}) present in the LKB1 A-loop is labeled. Secondary structure elements are labeled according to the structure of PKA (*15*).

assembly (Fig. 2B). Combining the His^{231}-Phe^{233} double mutant with the Tyr^{185} mutation that disrupts interaction with MO25α (*14*) resulted in a mutant STRADα that did not form a complex with LKB1 and MO25α (Fig. 2B). These experiments define the regions on STRADα that interact with LKB1 and MO25α and contribute to the assembly of an active LKB1 complex.

A common feature of many protein kinase folds is a C-terminal flanking tail (CFT) that interacts with the N-terminal lobe of the kinase (*18*). This tail either serves directly as an autoactivatory mechanism or provides a docking site for regulatory interacting partners (*18*). LKB1 has a proline-rich CFT_L (residues 311 to 347) that runs along the STRADα-LKB1 interface and interacts with the STRADα helix αG as well as the LKB1 N-terminal lobe (Fig. 1, A and C). An LKB1 mutant lacking part of the CFT_L motif (ΔCFT_L, residues 1 to 318) failed to interact with STRADα in the absence of MO25α (Fig. 2C). Mutation of individual residues in or interacting with the CFT_L (Trp^{332}, Tyr^{340}, and Arg^{74}) did not affect assembly of the LKB1 complex; however, LKB1(ΔCFT_L) formed a complex with reduced catalytic activity when coexpressed with STRADα and MO25α (Fig. 2D). As mentioned above, mutation of Arg^{74} (which interacts with the CFT_L but also with STRADα; Fig. 1, B and C) on LKB1 abolished interaction with STRADα in the absence of MO25α (Fig. 2C) and reduced the catalytic activity of the complex (Fig. 2D). The CFT_L also contains two phosphorylation sites: Ser^{325} (*19*), which may be phosphorylated by ERK (*20*), and Thr^{336}, an autophosphorylation site (*19*). These sites appear not to directly influence LKB1 catalytic activity (*19*) or complex assembly (*11*) but could affect association of LKB1 with substrates or regulators. These results reveal an important role for the CFT_L in LKB1-STRADα interactions and LKB1 activity and are suggestive of a potential role for other, as yet unidentified, LKB1 regulators that may make use of this region.

Most protein kinases are activated by phosphorylation of their activation loop, producing a conformation competent for substrate binding (*21*). Despite the lack of activating phosphorylation, the LKB1 activation loop is well ordered (fully defined by electron density) and adopts a conformation typical of loops from active protein kinases (Fig. 1A and fig. S6). Key to this is the interaction of Phe^{204} from the LKB1 activation loop with a hydrophobic pocket on the concave surface of MO25α (Fig. 1D). Individual mutation of Phe^{204} did not affect LKB1 complex formation or activity (Fig. 2D). However, mutation of Phe^{204} together with Arg^{74}, a residue required for LKB1-STRADα interaction (Figs. 1B and 2C), resulted in LKB1 species that were incapable of forming a heterotrimeric complex (Fig. 2D). Additional interactions occur between Arg^{240} and Phe^{243} on MO25α with the backbone of Ala^{205}

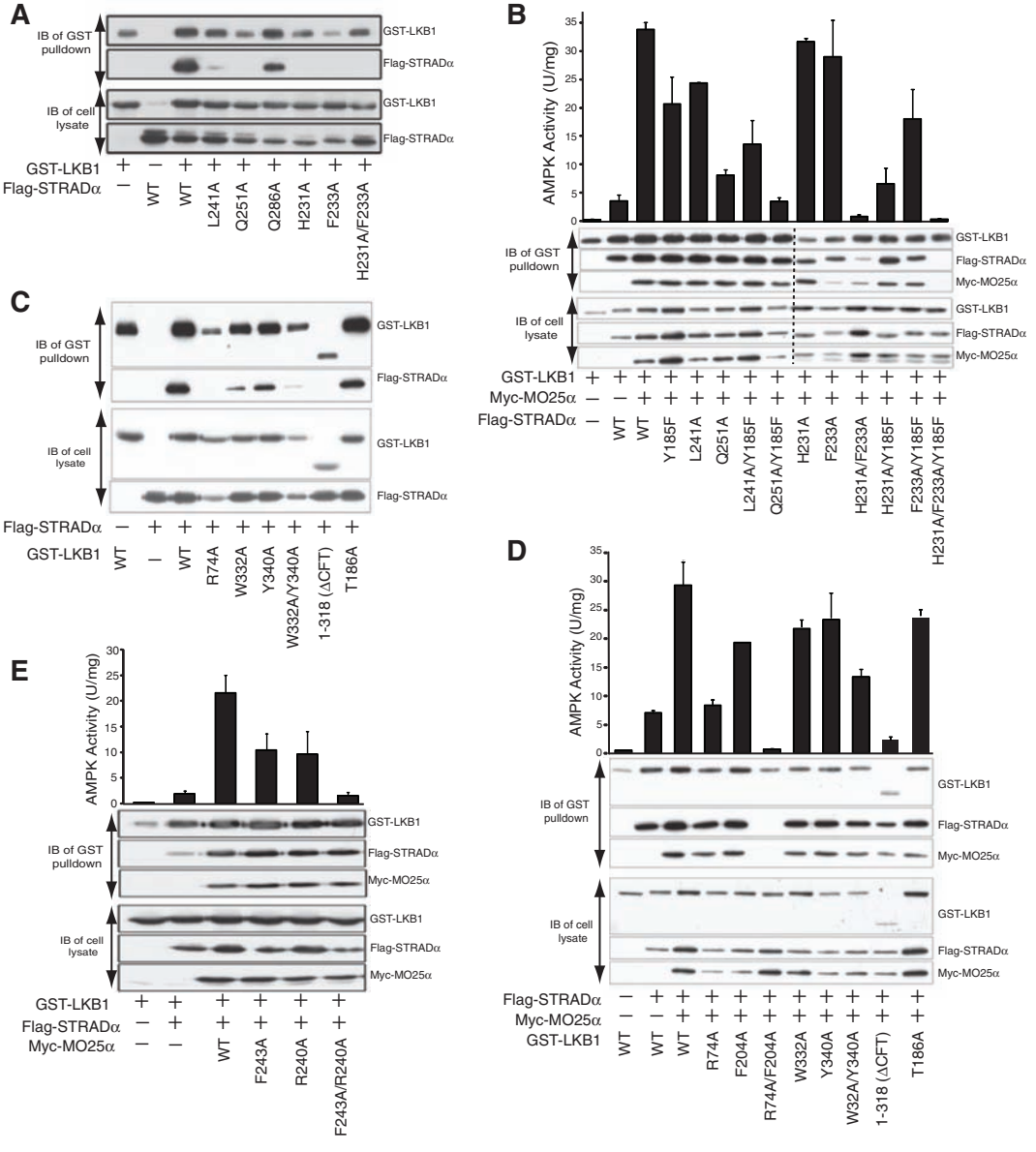

Fig. 2. Characterization of the LKB1-STRADα-MO25α interactions and LKB1 activation. (**A** and **C**) The indicated constructs of GST-LKB1 and Flag-STRADα were expressed in 293 cells in the absence of MO25α. Cells at 36 hours after transfection were lysed and GST-LKB1 was affinity-purified on glutathione-Sepharose. The purified GST-LKB1 preparation (upper panels) as well as the cell extracts (lower panels) were immunoblotted with the indicated antibodies. Similar results were obtained in three separate experiments. (**B**, **D**, and **E**) 293 cells were cotransfected with the indicated constructs of GST-LKB1, Flag-STRADα, and Myc-MO25α. Cells at 36 hours after transfection were lysed and GST-LKB1 was affinity-purified and assayed for the ability to activate heterotrimeric AMPK complex expressed in *Escherichia coli* (see supporting online material). Kinase activities are representative of three independent assays carried out in triplicate (error bars represent SD for a single triplicate experiment). Affinity-purified GST-LKB1 preparation (upper panels) as well as cell extracts (lower panels) were immunoblotted with the indicated antibodies.

and Ala^{206} of LKB1; Arg^{240} and Phe^{243} act as a molecular "peg" to orient the activation loop of LKB1 and stabilize its active conformation (Fig. 1D). Although mutation of both Arg^{240} and Phe^{243} did not affect the ability of MO25α to interact with STRADα and LKB1, the resulting complex is inactive, establishing the importance of this interaction in stimulating LKB1 (Fig. 2E). Although MO25α alone is known not to form a stable complex with LKB1 (*10*, *11*), in the presence of STRADα, MO25α stabilizes the activation loop of LKB1 in an optimal conformation required for phosphorylation of substrates. The position of Thr^{212} in the LKB1 activation loop is equivalent to that of the activation loop phosphothreonine of protein kinases that require activatory phosphorylation (Fig. 1E). However, Glu^{199} (β9) replaces the negative charge that would otherwise be provided by the phosphate group and is within hydrogen-bonding distance of Lys^{175} (Fig. 1E). A PJS mutation, Glu^{199} → Lys, impaired LKB1 catalytic activity, although a less severe PJS mutation (Glu^{199} → Gln) did not impair LKB1 activity (fig. S9).

Dozens of human genes code for protein kinases that lack essential residues in their catalytic machinery and have been termed pseudokinases (*22*, *23*). Some are in fact catalytically competent (*24*), but others are either incapable of binding ATP (*25*) or incapable of catalyzing phosphoryl transfer (*14*). It is possible that STRADα evolved from a catalytically competent protein kinase that phosphorylated LKB1. This notion is supported by the observation that STRADα interacts with LKB1 through structural elements in its C lobe that are normally used by active protein kinases to bind their substrates (e.g., the p+1 loop/αG helix). More important, protein kinases generally need to be in their active conformation to bind their substrates, and STRADα appears to adopt an "active" conformation stabilized through ATP and MO25 to activate LKB1 (*14*).

In order for LKB1 to phosphorylate AMPK, the active-site cleft of LKB1 must be accessible. Indeed, the structure of the heterotrimer shows that the C-terminal lobe of LKB1 is not engaged in interactions with STRADα or MO25α. Moreover, the region around the γ-phosphate (disordered in our structure) of ATP is solvent-exposed in LKB1 (fig. S7C).

Mutations in the gene encoding LKB1 are the main cause of PJS (*1*), and at least 51 missense mutations have been mapped to the LKB1 kinase domain and the CFT$_L$ loop (Fig. 3, table S2, and fig. S10). We have characterized the effects that these mutations have on the ability of LKB1 to form active heterotrimeric complexes with STRADα and MO25α (*11*) (fig. S9). The majority of mutations are residues important for the structural integrity of LKB1 (Fig. 3A). There are two hydrophobic clusters, named hydrophobic cluster 1 (Phe^{157}, Leu^{242}, Leu^{285}, Trp^{308}) and hydrophobic cluster 2 (Leu^{164}, Ile^{177}, and Leu^{182}) (Fig. 3A). Many of these mutations resulted in low LKB1 expression levels, and all of these LKB1 mutants were incapable of forming active complexes with

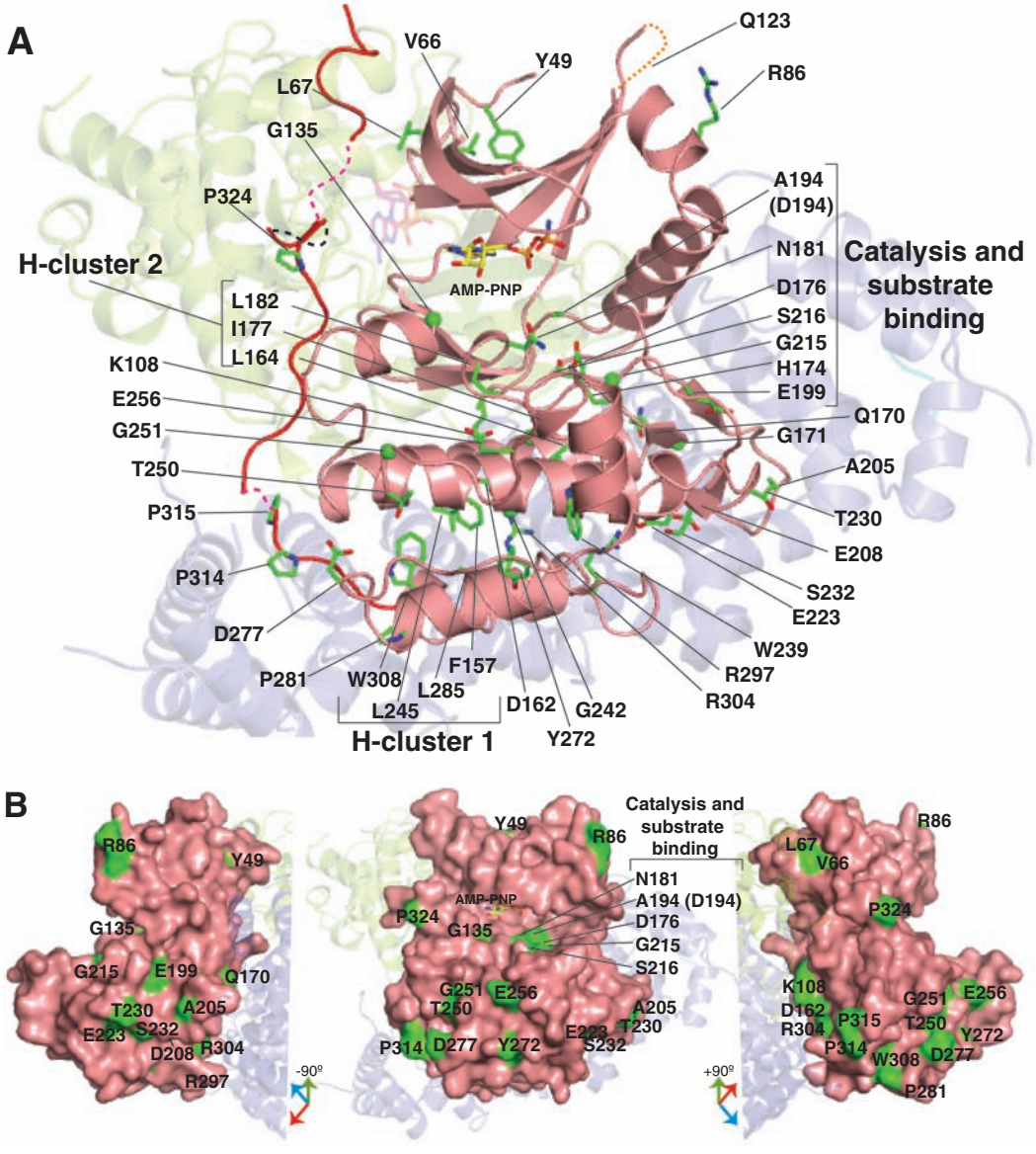

Fig. 3. Map of oncogenic mutations on the LKB1 kinase domain and the CFT$_L$. (**A**) Location of LKB1 residues that are mutated in PJS and other types of cancer. The CFT$_L$ region is colored red. Dashed lines represent areas that were not well defined by electron density. (**B**) Surface-exposed residues that are mutated in PJS and other types of cancer.

STRADα and MO25α (Fig. 3 and table S2). In addition, at least 10 mutations involve residues required for catalysis or substrate binding (Fig. 3). Although these mutants properly assembled into complexes with STRADα and MO25α, these were devoid of catalytic activity (fig. S9 and table S2). Other mutations present in the activation loop ($Ala^{205} \rightarrow Thr$, $Asp^{208} \rightarrow Asn$), the αEF-αF loop ($Thr^{230} \rightarrow Pro$, $Ser^{232} \rightarrow Pro$), and the CFT_L region ($Pro^{314} \rightarrow His$, $Pro^{315} \rightarrow Ser$, $Pro^{324} \rightarrow Leu$) did not affect the ability of LKB1 to assemble into active complexes. There are also a number of oncogenic mutations in solvent-exposed residues ($Arg^{86} \rightarrow Gly$, $Gln^{123} \rightarrow Arg$, $Tyr^{272} \rightarrow His$, $Asp^{277} \rightarrow Tyr$) that do not affect complex assembly or activity (fig. S9 and table S2). Thus, out of 51 mutations analyzed, 18 formed complexes with STRADα and MO25α that showed LKB1 activity (table S2). Assuming these are cancer-driving rather than passenger mutations, some of these mutations may be involved in interacting with other regulators or substrates of the LKB1 pathway.

Our study reveals how LKB1 is activated. In addition to STRADα binding, MO25α plays a crucial role in stabilizing the LKB1 activation loop in a conformation required for phosphorylation of substrates. Thus, a previously unrecognized role of STRADα is to promote interaction between MO25α and LKB1. This represents a mechanism by which kinases may be regulated allosterically, independent of activation loop phosphorylation. The LKB1 complex structure also shows how cancer mutations affect LKB1 function by impairing complex assembly, catalytic activity, and potential interactions with substrates or regulators. Finally, our findings provide insights into how certain pseudokinases may have evolved, by retaining active conformations that allow interactions similar to those by which active kinases bind their substrates.

References and Notes

1. A. Hemminki *et al.*, *Nature* **391**, 184 (1998).
2. H. Ji *et al.*, *Nature* **448**, 807 (2007).
3. R. J. Shaw, *Acta Physiol.* **196**, 65 (2009).
4. X. Huang *et al.*, *Biochem. J.* **412**, 211 (2008).
5. R. J. Shaw *et al.*, *Science* **310**, 1642 (2005).
6. B. Zheng, L. C. Cantley, *Proc. Natl. Acad. Sci. U.S.A.* **104**, 819 (2007).
7. A. F. Baas, L. Smit, H. Clevers, *Trends Cell Biol.* **14**, 312 (2004).
8. J. M. Lizcano *et al.*, *EMBO J.* **23**, 833 (2004).
9. A. F. Baas *et al.*, *EMBO J.* **22**, 3062 (2003).
10. J. Boudeau *et al.*, *EMBO J.* **22**, 5102 (2003).
11. J. Boudeau *et al.*, *J. Cell Sci.* **117**, 6365 (2004).
12. S. A. Hawley *et al.*, *J. Biol.* **2**, 28 (2003).
13. C. C. Milburn, J. Boudeau, M. Deak, D. R. Alessi, D. M. F. van Aalten, *Nat. Struct. Mol. Biol.* **11**, 193 (2004).
14. E. Zeqiraj *et al.*, *PLoS Biol.* **7**, e1000126 (2009).
15. D. R. Knighton *et al.*, *Science* **253**, 414 (1991).
16. A. C. Dar, T. E. Dever, F. Sicheri, *Cell* **122**, 887 (2005).
17. T. Rajakulendran, M. Sahmi, M. Lefrançois, F. Sicheri, M. Therrien, *Nature* **461**, 542 (2009).
18. N. Kannan, N. Haste, S. S. Taylor, A. F. Neuwald, *Proc. Natl. Acad. Sci. U.S.A.* **104**, 1272 (2007).
19. G. P. Sapkota *et al.*, *Biochem. J.* **362**, 481 (2002).
20. B. Zheng *et al.*, *Mol. Cell* **33**, 237 (2009).
21. B. Nolen, S. Taylor, G. Ghosh, *Mol. Cell* **15**, 661 (2004).
22. G. Manning, D. B. Whyte, R. Martinez, T. Hunter, S. Sudarsanam, *Science* **298**, 1912 (2002).
23. J. Boudeau, D. Miranda-Saavedra, G. J. Barton, D. R. Alessi, *Trends Cell Biol.* **16**, 443 (2006).
24. K. Mukherjee *et al.*, *Cell* **133**, 328 (2008).
25. E. D. Scheeff, J. Eswaran, G. Bunkoczi, S. Knapp, G. Manning, *Structure* **17**, 128 (2009).

26. We thank the European Synchrotron Radiation Facility, Grenoble, for beam time at station ID14-3 and T. J. Richmond and I. Berger (ETH Zürich) for providing the MultiBac expression vectors. Supported by a TENOVUS Scotland studentship (E.Z.), a Wellcome Trust Senior Research Fellowship (D.M.F.v.A.), the Medical Research Council (D.R.A.), Cancer Research UK grant C33794/A10969, and the pharmaceutical companies supporting the Division of Signal Transduction Therapy Unit (AstraZeneca, Boehringer-Ingelheim, GlaxoSmithKline, Merck & Co. Inc., Merck KgaA, and Pfizer). The coordinates and structure factors have been deposited with PDB entry 2WTK.

Supporting Online Material

www.sciencemag.org/cgi/content/full/1178377/DC1
Materials and Methods
Figs. S1 to S12
Tables S1 and S2
References

29 June 2009; accepted 20 October 2009
Published online 5 November 2009;
10.1126/science.1178377
Include this information when citing this paper.

The Subtle Transmission of Race Bias via Televised Nonverbal Behavior

Max Weisbuch,* Kristin Pauker, Nalini Ambady*

Compared with more explicit racial slurs and statements, biased facial expressions and body language may resist conscious identification and thus produce a hidden social influence. In four studies, we show that race biases can be subtly transmitted via televised nonverbal behavior. Characters on 11 popular television shows exhibited more negative nonverbal behavior toward black than toward status-matched white characters. Critically, exposure to prowhite (versus problack) nonverbal bias increased viewers' bias even though patterns of nonverbal behavior could not be consciously reported. These findings suggest that hidden patterns of televised nonverbal behavior influence bias among viewers.

In contemporary Western culture, most people claim that they do not behave in a racially biased fashion, and America recently elected its first black president. Yet recent claims of a race-blind society are contradicted by studies of race biases, in which people exhibit more positive responses to one race than another (*1*–*6*). To the extent that race biases are communicated explicitly, egalitarian norms encourage observers to discount them as a valid source of knowledge (*7*, *8*). For example, observers can consciously debate and publicly denounce race-biased aggressive acts, verbal statements, and hiring procedures, thus resisting conformity to these explicit race biases. However, race biases are often communicated subtly via facial expressions and body language (*2*–*6*). Indeed, mounting evidence suggests that Americans' nonverbal behavior favors white over black persons (*2*, *4*, *9*–*12*). Because nonverbal behavior is "off the record" and can be difficult to identify unambiguously, exposure to nonverbal race bias may undermine norm-driven correction processes and hence may exert a social influence (*13*, *14*). Specifically, exposure to nonverbal race bias, via evaluative conditioning, may cause perceivers to associate race with affect and thus exhibit race bias themselves (*15*–*18*). We examined the prevalence, subtlety, and impact of nonverbal race bias in four studies. We observed that nonverbal race bias occurs on television and that exposure to this televised bias accounts in part for white viewers' own race bias, as assessed with reaction-time and self-report measures. Moreover, patterns of nonverbal bias were influential even when they could not be consciously reported.

Table 1. Study 1: Featured (but unseen) character ratings by race. Means ± SD; *t*(28).

Character rating	White character mean	Black character mean	*t* value	*P* value	*rpb*
Favorable nonverbal response	0.16 ± 0.24	−0.04 ± 0.28	2.08	0.047*	0.37
Favorable verbal response	0.17 ± 0.20	0.04 ± 0.34	1.35	0.19	0.25
Perceived attractiveness	4.88 ± 1.16	4.74 ± 1.04	0.35	0.73	0.07
Perceived sociability	4.79 ± 0.66	5.14 ± 0.88	−1.22	0.23	0.22
Perceived kindness	4.54 ± 0.77	4.75 ± 0.48	−0.90	0.38	0.17
Perceived intelligence	4.92 ± 1.05	5.12 ± 0.93	−0.56	0.58	0.10

Department of Psychology, Tufts University, 490 Boston Avenue, Medford, MA 02155, USA.

*To whom correspondence should be addressed. E-mail: max.weisbuch@tufts.edu (M.W.); nalini.ambady@tufts.edu (N.A.)